

# A Novel Colored Fluid Stochastic Petri Net Simulation Model for Reliability Evaluation of Wind/PV/Diesel Small Isolated Power Systems

Yiannis A. Katsigiannis, Pavlos S. Georgilakis, *Member, IEEE*, and George J. Tsinarakis, *Member, IEEE*

**Abstract**—This paper introduces a new general methodology for the modeling and reliability evaluation of small isolated power systems, which include wind turbines, photovoltaics, and diesel generators, based on fluid stochastic Petri nets (FSPNs). The proposed methodology presents two major novelties in FSPN modeling, namely: 1) the introduction of a new kind of Petri net arc, called the database arc, which makes possible the direct import of real data in the simulation process; and 2) the selection of constant time intervals in FSPN modeling, instead of assuming continuous dynamics defined by the change of fluid level over time. Moreover, in order to construct the overall system model, this paper proposes a general framework for modular representation of the system under study following a number of well-defined steps. The obtained model is fully parameterized and compared to classical simulation methods, it provides to its user the additional advantage of graphical representation of system's components and attributes. Four scenarios, which describe power system's performance under different conditions, were implemented. For each one of the developed scenarios, nine reliability and performance indexes have been calculated and compared.

**Index Terms**—Fluid stochastic Petri nets (FSPNs), hybrid systems, photovoltaics (PVs), reliability evaluation, renewable energy sources (RES), simulation, small isolated power systems (SIPS), wind turbines (WTs).

## LIST OF ACRONYMS AND SYMBOLS

### Acronyms

SIPS	Small isolated power systems.
RES	Renewable energy sources.
DG	Diesel generator.
WT	Wind turbine.
PV	Photovoltaic.
PN	Petri net.
CPN	Colored Petri net.
FSPN	Fluid stochastic Petri net.
LOEE	Loss of energy expectation.
EIU	Energy index of unreliability.

DGEP	DG energy produced.
MTTF	Mean time to failure.
MTTR	Mean time to repair.
TTF	Time to failure.
TTR	Time to repair.
STC	Standard test conditions for PVs.

### Symbols

$P$	Set of FSPN places.
$P_d$	Subset of FSPN discrete places.
$P_c$	Subset of FSPN continuous places.
$T$	Set of FSPN transitions.
$T_e$	Subset of FSPN stochastically timed transitions.
$T_i$	Subset of FSPN immediate transitions.
$A$	Set of FSPN arcs.
$A_n$	Subset of FSPN normal arcs.
$A_i$	Subset of FSPN inhibitor arcs.
$A_t$	Subset of FSPN test arcs.
$A_{db}$	Subset of FSPN database arcs.
$B$	Function that describes the upper bound of tokens on each FSPN place.
$W$	Weight function that refers to FSPN arc weights.
$M_0$	Initial state of FSPN.
$p_i$	Place $i$ of FSPN.
$t_i$	Transition $i$ of FSPN.
$M_{P_i}$	Marking of place $p_i$ .
$\Sigma$	Finite set of nonempty types (color sets) of a CPN.
$C$	Color function of a CPN.
$G$	Guard function of a CPN.
$Cont.$	Continuous FSPN place.
$Disc.$	Discrete FSPN place.
$P_R$	Rated power of WT.
$V$	Wind speed.
$V_{in}$	Cut-in speed of WT.
$V_{out}$	Cutout speed of WT.
$P_{WT}$	WT generated power.
$k_W$	Shape factor of Weibull distribution.
$c_W$	Scale factor of Weibull distribution.
$\bar{V}_{annual}$	Mean annual wind speed.
$rnd(0, 1)$	Uniformly distributed random number generation function in the interval (0, 1).
$P_{PV}$	Power of the PV array.
$\eta_{inv}$	Inverter efficiency.
$f_{PV}$	PV derating factor.
$P_{STC}$	Nominal PV array power.

Manuscript received February 17, 2007; revised December 13, 2007, October 31, 2008, April 14, 2009, and November 10, 2009. Date of publication August 9, 2010; date of current version October 15, 2010. This work was supported in part by the European Commission under contract FP6-INCO-CT-2004-509205 (VBPC-RES project). This paper was recommended by Associate Editor M. Jeng.

Y. A. Katsigiannis and G. J. Tsinarakis are with the Department of Production Engineering and Management, Technical University of Crete, 73100 Chania, Greece (e-mail: katsigiannis@dpem.tuc.gr; tsinar@dpem.tuc.gr).

P. S. Georgilakis is with the School of Electrical and Computer Engineering, National Technical University of Athens, 15780 Athens, Greece (e-mail: pgeorg@power.ece.ntua.gr).

Digital Object Identifier 10.1109/TSMCA.2010.2052607

$G_A$	Global solar radiation incident on the PV array.
$G_{STC}$	Solar radiation under STC (1 kW/m <sup>2</sup> ).
$T_c$	Temperature of the PV cells.
$T_{STC}$	STC temperature (25 °C).
$C_T$	PV temperature coefficient.
$T_a$	Ambient temperature.
$G$	Global solar radiation on a horizontal plane.
$NOCT$	Normal operating PV cell temperature.

## I. INTRODUCTION

A SMALL isolated power system (SIPS) presents some unique characteristics that are related with its distance from the electrical grid and the small amount of load that it has to serve. Renewable energy sources (RES) are often present in geographically remote and demographically sparse areas, so they can be used as an energy source in SIPS. However, since renewable technologies depend on a resource that is not dispatchable [1], they are used as a supplementary energy source working in parallel with dispatchable units, such as diesel generators (DGs), in order to save fuel. The primary choices of RES technologies in SIPS are usually wind turbines (WTs) and photovoltaics (PVs). The combination of WTs and PVs may improve their individual performance by attenuating the resulting fluctuations, increasing the overall energy output, and reducing furthermore fuel consumption.

For the reliability evaluation of SIPS, mainly deterministic techniques have been applied such as: 1) the loss of largest unit; 2) a fixed percent margin; or 3) a combination of the previous two methods. However, these techniques do not define consistently the true risk of the system, as they can lead to very divergent risks even for systems that are very similar. This characteristic makes the provided results unreliable in many cases. In addition, these techniques cannot be extended to include intermittent sources, such as wind and solar energy [2]. Besides the deterministic techniques, the other two basic approaches for reliability evaluation of power systems are the direct analytical methods and the Monte Carlo simulation. Most of the published work in SIPS that contain wind energy conversion systems is focused on the use of analytical methods [3], [4] which, however, cannot recognize completely the chronological variation of wind and its effect in the operation of SIPS that contain WTs or PVs.

Petri nets (PNs) are a graphical and mathematical tool originally developed for the modeling and analysis of distributed systems and in particular for the notions of concurrence, non-determinism, communication, and synchronization. One of the main advantages of PNs as a modeling tool is that they have very few, but powerful, primitives that make them relatively easy to apply. Extension of their use for dynamic systems modeling made necessary the introduction of time delays, leading to the definition of (deterministic) timed PNs and stochastic PNs [5], which are useful for performance evaluation (manufacturing systems [6], [7], computer systems [8], etc.). Moreover, the high complexities of such systems guided to abbreviations of the original graphical representation of PNs. Colored PNs (CPNs) [9] belong to this category, as with the use of colors, the modeling of complex systems with repeated structural parts

can be significantly simplified, maintaining at the same time the discrete character of the tool. To enhance the application of PNs in the field of continuous systems, several extensions and variations were introduced, with most important hybrid PNs [10], [11] and fluid stochastic Petri nets (FSPNs) [12]. These PN variations combine both continuous and discrete components and thus can describe hybrid systems, such as power systems. In this paper, the FSPN model has been selected, since it concentrates on the evolution of the stochastic process involved [13]. This makes it appropriate for power systems simulation, especially in the case that they include a large number of stochastic variables (e.g., SIPS containing RES technologies).

PNs combine the characteristics of simulation methods with the additional advantage of graphical representation. Moreover, PNs contain a complete collection of analysis tools which can be used for the detection of a number of structural properties that are useful for the behavioral and quantitative analysis of the system. Compared to classical simulation methods, PNs incorporate significant advantages such as absence of logical errors and deadlocks, impossibility of reaching catastrophic states, and inherent concurrence [14].

Another attractive feature of PNs is that they can be used for hierarchical representation of complicated systems. Hierarchical methods refer to the reduction of a complicated problem in a number of simpler approximative subproblems which can be solved, and their solutions are appropriately combined to produce the overall problem solution. The main reasons that make the application of such an approach necessary are, namely: 1) the interactions between the systems components; 2) the extensive number of events taking place in a system of real complexity; and 3) the information exchange between them. Two families of hierarchical approaches are met in the bibliography: a) simplification of the implemented models by reducing the considered details; and b) synthesis techniques based on the use of modular subsystems. Modular-based techniques are further divided into two subcategories, namely: top-down synthesis and bottom-up synthesis. In the first case, a model is built, and through an iterative process, details are added to it, while in the second case, the overall system is decomposed into subsystems, the PN model of each subsystem is implemented, and synthesis techniques are used to construct the PN model of the overall system.

The features described earlier verify the suitability of PNs for the modeling of reliability and safety scenarios in engineering systems [15]. In power systems area, PNs have been used for reliability evaluation and fault diagnosis, mainly in transmission and distribution systems [16]–[18]. In power generation, PNs have been used in the analysis of grid-connected systems [19], [20], isolated systems [21], as well as on the temperature control of a cogenerative plant [22]. However, the examined types of systems described contain only conventional energy sources, so modeling of RES technologies seems to be a new task.

This paper proposes a reliability evaluation simulation model for SIPS based on FSPNs. The proposed methodology considers subsystem models that are structurally and functionally connected appropriately using common structural elements (common places or transitions). In addition, the methodology is

of general use and makes possible the construction of the model and the calculation of its necessary parameters according to the given characteristics, following a number of well-defined steps. Moreover, instead of considering continuous dynamics defined by the change of fluid level over time as in the bibliography, a novel approach that assumes constant time intervals is adopted here, and the most important quantitative and qualitative characteristics of a system's operation are studied. The examined SIPS can contain one or more WTs, a PV array, and a DG, while the calculations are performed on an hourly basis, in order to take into account the variations of wind speed and load demand in SIPS performance. The load consumption is derived from an hourly load profile that is inserted in the proposed FSPN with the help of the database arcs that are introduced in this paper.

A major advantage of the proposed methodology is that the PN model is very flexible, since several of its variables are parameterized (can take alternative values). These variables include simulation duration, peak load, WT, PV and DG technical characteristics, as well as failure and maintenance durations. Another benefit arising from the use of the proposed methodology is that it can be treated in two ways, namely: as a typical simulation procedure, as well as a combination of graphical and mathematical representation of SIPS operation state. Thus, the proposed methodology can be used either by SIPS planners and designers for the evaluation of different system configurations, or by SIPS operators for the simulation of a system's operation and the examination of a system's performance under several operating states including extraordinary conditions. In order to investigate the flexibility and the capabilities of the proposed methodology, a base scenario has been considered that contains one WT, a PV array, and one DG. Then the results of the base scenario are compared with the results provided by the same FSPN under three different scenarios, namely: 1) adding a smaller WT in the system; 2) existence of lower wind potential; and 3) increasing DG capacity. The evaluation of each examined scenario is based on the calculation of five reliability and four performance indexes.

This paper is organized as follows: Section II presents the basic reliability indexes and energy quantities that are used in the study of hybrid SIPS containing WTs and PVs. Section III contains a brief description of FSPNs. Section IV introduces the database arcs that are used so as to import more precise data in the simulation process modeled by the PN. Section V analyzes the structure of the proposed FSPN, and Section VI presents and discusses the obtained results. Section VII concludes the paper.

## II. RELIABILITY AND PERFORMANCE INDEXES

The basic *reliability indexes* that can be obtained through the simulation of the considered SIPS are listed as follows [23]:

- 1) Loss of load probability (LOLP), which is defined as the probability that the load will exceed available generation.
- 2) Loss of load expectation (LOLE), i.e., the expected hours per year during which a system capacity shortage occurs.
- 3) Loss of energy expectation (LOEE), which represents the expected energy not supplied by the generating units per year.





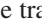
- 4) Energy index of unreliability (EIU) that normalizes LOEE by dividing it with the annual energy demand.
- 5) Frequency of interruptions (FOI), i.e., the expected number of times that loss of load occurs per year.


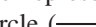

The knowledge of the above five indexes leads to the estimation of numerous other reliability indexes [23]. In addition, the following four *performance evaluation indexes* are computed:

- 6) Wind energy production (WEP) from WTs expressed in kWh.
- 7) Surplus energy (SE), which expresses the amount of energy (in kWh) generated from WTs and PVs that was available but not utilized.
- 8) Capacity factor (CF) that expresses the actual energy output of WT for a year divided by the energy output if WT operated at its rated power output for the entire year.
- 9) Diesel generator energy production (DGEP), expressed in kWh.

## III. FSPNs

The FSPNs used in this paper arise from the FSPN definition presented in [24] by adapting certain features according to the desired behaviors. An FSPN is defined as  $FSPN = \{P, T, A, B, W, M_0\}$ , where  $P$  is the set of places partitioned into the subset of discrete places  $P_d$  and the subset of continuous places  $P_c$ , and  $T$  is the set of transitions partitioned into the subset of stochastically timed transitions  $T_e$  and the subset of immediate transitions  $T_i$ . The set  $A$  of arcs is partitioned into four subsets, namely: the subset  $A_n$  of normal arcs, the subset  $A_i$  of inhibitor arcs, the subset  $A_t$  of test arcs, and the subset  $A_{db}$  of database arcs. In a PN, transitions and places are connected through arcs interchangeably. A transition without an input place is called a source transition, while a transition without any output places is a sink transition. Function  $B$  describes the upper bound of tokens on each place. The weight function  $W$  refers to arc multiplicity weights and can be a constant number, a mathematical function, or a function of certain places' markings. Finally, the initial state of FSPN is denoted by  $M_0$ .

In an FSPN, discrete places are drawn as simple circles  and continuous places as double circles . The lower bound of each discrete place marking is zero, while continuous places can have a negative marking. The presence of a negative marking in a continuous place does not change the fundamental firing rule of PNs. Immediate transitions are represented as black bars , and timed transitions (either deterministic or stochastic) are represented as empty bars . In case of structural conflicts, priorities in the firing of the transitions can be defined. The default priority for a transition is one, while transitions with higher priorities are represented with the typical bar symbol, containing their priority index (e.g., ).

Normal arcs are drawn as usual arcs ()>, inhibitor arcs are represented by arcs whose end is marked with a small circle ()>, while test arcs are represented by arcs with dotted lines (). The use of these arc extensions increases significantly the modeling capabilities of a PN. If a place  $p$  and a transition  $t$  are connected with an inhibitor arc with weight

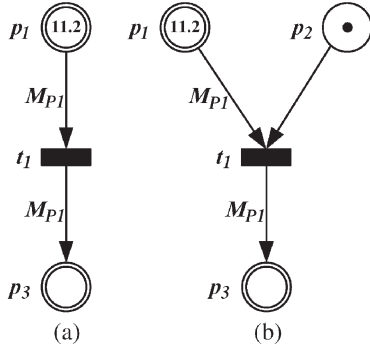


Fig. 1. Firing control of an immediate transition when it is combined with a continuous input place.

$w$ ,  $t$  can only fire if the marking of  $p$  is less than  $w$ . On the contrary, if  $p$  and  $t$  are connected with a test arc with weight  $w$ ,  $t$  can only fire if the marking of  $p$  is greater than or equal to  $w$ . After the firing process, the marking of  $p$  remains unchanged since no tokens are removed through inhibitor and test arcs. For complete information about enabled conditions and firing sequence in PN models that contain discrete and continuous nodes, the reader is referred to [25].

In FSPNs the study of a hybrid system's continuous part is performed by assuming rates equal to arc weights that connect continuous places and timed transitions. The product of the arc's weight with the time duration of its related transition is equal to the fluid level change. However, in SIPS simulation models (such as HOMER [26] and HYBRID2 [27]), constant time intervals—mainly hourly—are considered, and during them, the input and output variables of the system are supposed to be constant. The operation of the proposed FSPN follows this approach. Places are used to calculate the basic characteristics of SIPS operation. Continuous places are used for the calculation of variables taking as values real numbers, while discrete places are used for the calculation of variables taking as values positive integers, as well as for the control of transitions firings. In the whole PN model of Section V, there is only one deterministic timed transition with duration equal to the selected time interval. The remaining transitions are immediate, and the simulation exploits the structural PN's properties of concurrence and parallelism to proceed. Arc weights are used for the calculations of studied characteristics, and quite often their value is a function of a place marking.

The use of continuous places as exclusive inputs to immediate transitions results in an event that keeps reoccurring with a probability equal to one. This function is depicted in Fig. 1(a), where  $t_1$  fires infinitely; in the first firing,  $t_1$  removes the fluid from  $p_1$ , and then it continues to fire with zero fluid. The symbol  $M_{p_i}$  related to certain arcs denotes that these arc weights are equal to the marking of place  $p_i$ . The modeling of the same situation according to Fig. 1(b) solves the problem. Transition  $t_1$  fires as many times as the number of tokens in  $p_2$ . Moreover, the presence of  $p_2$  gives to the PN user additional qualitative information related to the frequency that an event occurs, in parallel with the quantitative information that the continuous place provides.

Fig. 2 presents a simple example that is equivalent with an IF statement. The presence of discrete place  $p_2$  is essential

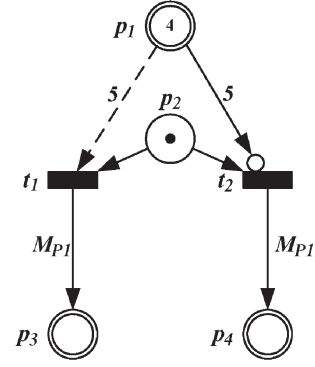


Fig. 2. Implementation of IF condition using inhibitor and test arcs.

for the firing of the transition that satisfies the true condition. For markings of  $p_1$  less than five (that is the arc weight of the inhibitor arc),  $t_2$  fires, while for markings of  $p_1$  greater than or equal to five (that is the arc weight of the test arc),  $t_1$  fires.

The definition of CPNs adds into the tuple of an ordinary PN the quantities  $\Sigma$ ,  $C$ , and  $G$ . More specifically,  $\Sigma$  is a finite set of nonempty types, also called color sets,  $C$  is a color function that is defined from the set of places  $P$  to  $\Sigma$ , while  $G$  is a guard function that maps each transition into a Boolean expression where all variables have types that belong to  $\Sigma$ . For more information about the problem of introducing colors in fluid systems, the reader is referred to [28]. It should be noticed that in the developed simulation model, different colors are considered as a graphical abbreviation in parts of the PN that do not contain timed transitions. Therefore, the use of CPNs is equivalent with a DO loop in these parts.

#### IV. DEFINITION OF DATABASE ARCS

In a PN simulation, it is possible that some variables, represented by places, have to take specific values that either cannot be modeled in a PN environment, or their modeling will increase significantly the graphical complexity of the system. For example, in order to examine the performance of SIPS for a specific hourly load profile of a year (8760 values), large numbers of places and arcs must be added to the PN for obtaining the desired load value for each hour. The increase of structural complexity in a PN leads to significant problems such as state space explosion, increase of the overall computational complexity, and increase of the simulation running time. For the solution of such problems, the concept of database arcs is introduced in this paper.

A database arc is connecting an immediate or timed transition, which has only one input place, with a continuous or discrete place. The weight of a database arc can take values that are included in a given matrix and is symbolized with  $\left[ \begin{smallmatrix} \text{A} \\ \text{---} \end{smallmatrix} \right]$ , where  $A$  is the name of the input matrix. A database arc is defined by its *dimension number* and its *input place*. The dimension number refers to the dimension of the input matrix  $A$ . For example, a column vector has a dimension equal to one; a 2-D matrix has a dimension equal to two, etc. The input place is always of discrete type, and it refers to the input place of the transition that is connected with the database arc. The marking of the input place shows the position of the element in  $A$  that



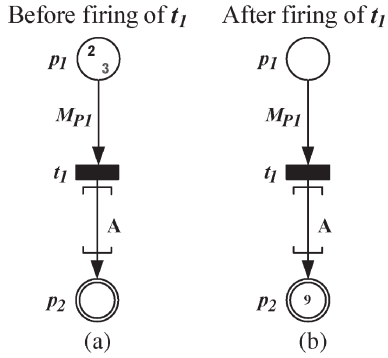


Fig. 3. Operation of database arcs.

is desirable to be imported in the considered analysis. If the dimension number is greater than one, the input place contains tokens of different colors. In that case, each color represents a different dimension of the input matrix. The correspondence between a specific color and the dimension number is common for all database arcs of the PN model.

Due to its discrete type, the input place of a database arc has a lower bound equal to zero and can enable its output transition if the marking is greater than zero. After the firing process, its marking becomes equal to zero, and the transition can fire again only if its input place is refilled. Moreover, an upper bound is associated with the input place of database arcs which depends on the number of elements of input matrix in each one of their dimensions. In case that the marking of the input place exceeds its upper bound, the transition is not firing. On the other hand, care must be also taken at the destination place of a database arc if this place has a finite capacity. Among the several strategies that have been proposed in the literature [29], the clamping strategy is adopted here, which truncates the marking of the place to the specified capacity.

Fig. 3 shows an example of graphical modeling and operation of a database arc. For this example, it is considered that the database arc obtains values from matrix  $A$

$$A = \begin{bmatrix} 2 & 0 & -12.4 & \cos(\pi/4) \\ 6.98 & \ln(5) & 9 & 37 \\ -\sqrt{3} & 74 & -42 & \exp(3) \end{bmatrix}. \quad (1)$$

The database arc that is depicted in Fig. 3 has dimension number equal to two, since matrix  $A$  is 2-D, while the input place  $p_1$  contains tokens of two colors. For clarity reasons, the marking of  $p_1$  that corresponds to the desired row of  $A$  is represented in black, and the marking of  $p_1$  that corresponds to the desired column of  $A$  is represented in gray. Fig. 3(a) shows the state of the PN before the firing of  $t_1$ , from which it can be observed that the requested element can be found in the second row and third column of  $A$ . Fig. 3(b) shows the state of the PN after the firing of  $t_1$ , in which the place  $p_2$  has a marking value of nine, since  $A(2, 3) = 9$ . After the firing of  $t_1$ , the input place  $p_1$  does not contain tokens in both colors.

Following this methodology, it is possible to retrieve the desired value of a matrix by putting the appropriate marking in the input place. For example, the PN model can be adjusted to export sequentially the elements of a row, a column, a diagonal, or to make a random selection. The use of database arcs can

be very helpful in the following situations especially when the number of data is large:

- 1) when it is desirable to import data that have to take specific values in a given sequence (e.g., meteorological data, network and automotive systems traffic data, biology data, sensor data, etc);
- 2) when the data do not follow any typical probability distribution function.

## V. WT/PV/ DG SIPS MODELING WITH FSPNs

This section describes the application of the proposed FSPN methodology for the modeling and hourly simulation of a SIPS that contains WTs, PV arrays, and DG. The developed model is taking into account the load demand, the wind speed variation, the WT power generation, the PV power generation based on radiation and temperature data, and the DG operation. Moreover, the evaluation of SIPS is achieved with the calculation of the reliability and performance indexes described in Section II. All the necessary simulations were implemented using Visual Object Net PN simulation package [30].

The main steps of the proposed methodology are depicted in Fig. 4. Following this process, the user constructs the overall FSPN model safely and effectively, independently of the complexity of the studied system. The overall system is divided into a finite number of fundamental subsystems according to the characteristics of the studied SIPS. The FSPN models of these subsystems are constructed, analyzed for their behavioral properties, and appropriately connected according to the considered topology and subsystems interaction in order to form the overall FSPN model. Then, the quantitative parameters are added to make it functional. The results obtained by the proposed FSPN are compared with the respective results of Monte Carlo simulation. By validating the FSPN model, it is ensured that it can be applied for the simulation of alternative scenarios.

The structure of the proposed FSPN, shown in Fig. 5, can contain six fluid stochastic Petri subnet (FSPsN) models, namely: 1) the input layer FSPsN that contains time information and parameter values; 2) the load demand FSPsN that imports load data to the model; 3) the WT FSPsN that simulates the WT operation; 4) the PV FSPsN that simulates the PV operation; 5) the diesel generator FSPsN that simulates the DG operation; and 6) the output layer FSPsN that calculates reliability and performance indexes. The interactions between the six FSPsN are also depicted in Fig. 5 with the help of arcs that connect them.

The four intermediate modules (WT, PV, load, and DG) of the proposed FSPN of Fig. 5 calculate the supply and demand of energy. The load model imports load data with the use of database arcs. The WT model contains the simulation procedure of one or more WTs. In case of existence of two or more WTs, a CPN is used, and each WT is represented with a different color. The PV model imports temperature and solar radiation data via database arcs and calculates the output of the PV array. The diesel generator model simulates the operation and maintenance of the DG. The WT and PV models are used as input to the DG module (Fig. 5), as the considered dispatch strategy presupposes the use of all wind energy produced and PV energy before DG serves the remaining load. Although the

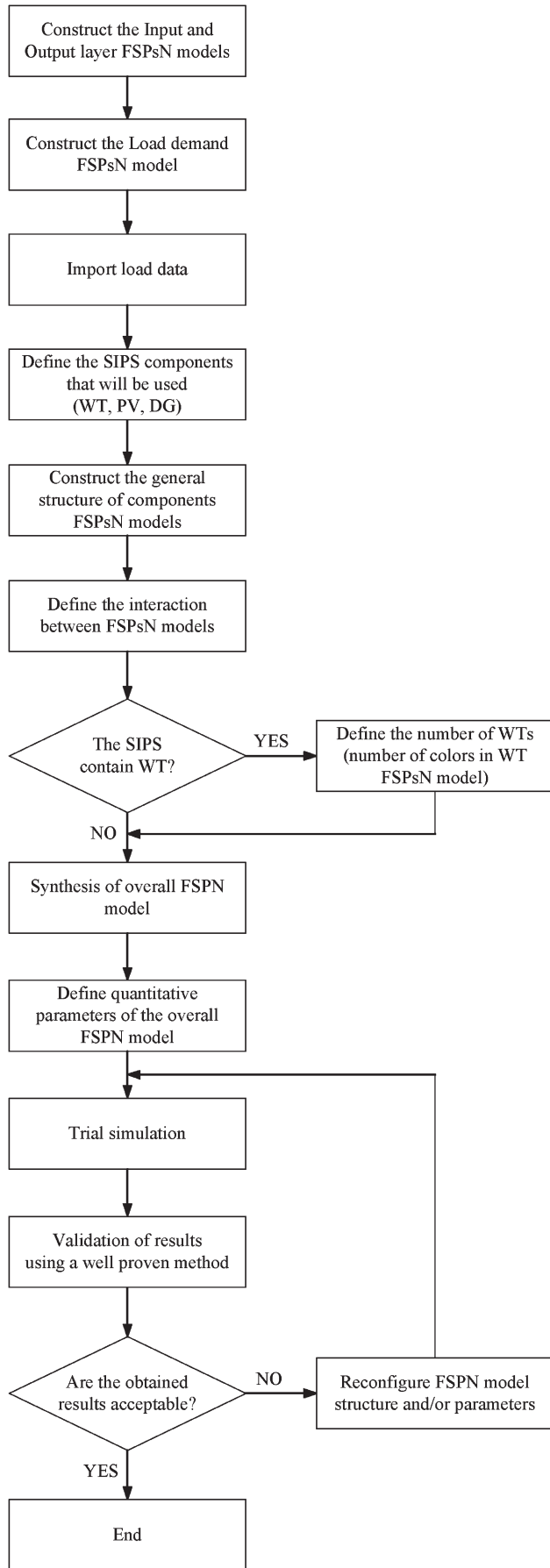


Fig. 4. Main steps of the proposed FSPN methodology.

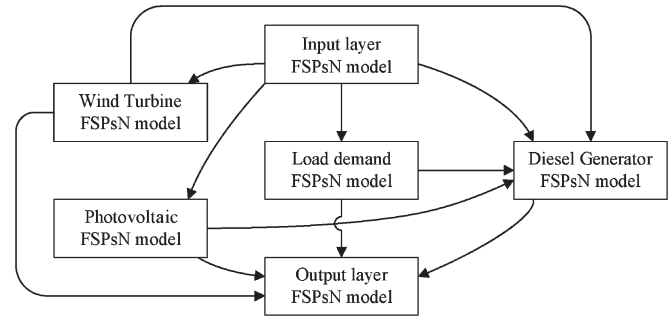


Fig. 5. Structure of the proposed FSPN for SIPS modeling.

TABLE I  
DESCRIPTION AND INITIAL VALUES OF INPUT LAYER PLACES

Place	Description	Type	Initial Value
$p_{in1}$	Number of simulation years	Disc.	500
$p_{in2}$	Remaining hours of the year	Disc.	8760
$p_{in3}$	Current hour of the year	Disc.	0
$p_{in4}$	Annual peak load demand	Cont.	25.00 kW
$p_{in5}$	Shape factor of Weibull distribution	Cont.	2.00
$p_{in6}$	Mean annual wind speed	Cont.	7.00 m/s
$p_{in7}$	Number of WTs	Disc.	1
$p_{in8}$	Rated power of WT, $P_R$	Cont.	20.00 kW
$p_{in9}$	Cut-in speed of WT, $V_{in}$	Cont.	3.00 m/s
$p_{in10}$	Rated speed of WT, $V_R$	Cont.	11.00 m/s
$p_{in11}$	Cut-out speed of WT, $V_{out}$	Cont.	22.00 m/s
$p_{in12}$	Coefficient $a$ of WT, eq. (2)	Cont.	2.49
$p_{in13}$	Coefficient $b$ of WT, eq. (2)	Cont.	-1.74
$p_{in14}$	Coefficient $c$ of WT, eq. (2)	Cont.	0.30
$p_{in15}$	Mean time to failure for WT	Disc.	1920 h
$p_{in16}$	Mean time to repair for WT	Disc.	80 h
$p_{in17}$	Nominal power of PV array, $P_{STC}$	Cont.	20 kW <sub>peak</sub>
$p_{in18}$	Nominal operating PV cell temperature, $NOCT$	Cont.	48°C
$p_{in19}$	Inverter efficiency, $\eta_{inv}$	Cont.	0.90
$p_{in20}$	PV derating factor, $f_{PV}$	Cont.	0.90
$p_{in21}$	PV temperature coefficient, $C_T$	Cont.	-0.004 /°C
$p_{in22}$	Maximum power of DG	Cont.	18.00 kW
$p_{in23}$	Scheduled maintenance of DG	Disc.	1000 h of operation
$p_{in24}$	Lower bound of DG maintenance duration	Disc.	2 h
$p_{in25}$	Upper bound of DG maintenance duration	Disc.	24 h
$p_{in26}$	Starting failure probability of DG	Cont.	0.01

proposed PN simulates the entire year, with only a few modifications it can be used to examine the results for a specific period of the year (summer period, specific months or weeks, etc.).

A brief description for each one of the six FSPsN models of Fig. 5 follows. For simplicity, when there is a connection between FSPsN models, only their direct connected parts with the described FSPsN are depicted.

#### A. Input Layer FSPsN Model

For the flexible parameterization of the system, the input layer of the proposed FSPN of Fig. 5 contains all the values that can be modified by the user in order to evaluate the performance of SIPS under different conditions. The places that are used as parameters, their type [either continuous (*Cont.*) or discrete (*Disc.*)] and their initial values are presented in Table I. All these places are connected, with the help of test arcs, with the

rest modules of the model (i.e., they remain unchanged during the whole simulation period), with the exception of places describing simulation time ( $p_{in1}$ ,  $p_{in2}$ , and  $p_{in3}$ ). Moreover, the input layer consists of three transitions, namely: 1) the immediate transition  $t_{in1}$ , which is needed for the conversion of the simulation years (place  $p_{in1}$ ) to the remaining hours of a year (place  $p_{in2}$ ); 2) the timed transition  $t_{in2}$ , which represents the hourly time step of the simulation; and 3) the immediate transition  $t_{in3}$ , which is the input transition for all the places that their marking is calculated via database arcs. Finally, a discrete place named  $p_{in27}$  is also contained in order to ensure the proper firing of  $t_{in1}$ .

WTs are modeled using

$$P_{WT}(V) = \begin{cases} 0 & V < V_{in} \\ a + b \cdot V + c \cdot V^2 & \text{for } V_{in} \leq V < V_R \\ P_R & V_R \leq V \leq V_{out} \\ 0 & V > V_{out} \end{cases} \quad \begin{matrix} (a) \\ (b) \\ (c) \\ (d) \end{matrix} \quad (2)$$

where  $P_{WT}$  is WT generated power,  $V$  is the wind speed,  $P_R$  is the rated power of WT,  $V_{in}$  is the cut-in speed,  $V_R$  the rated speed, and  $V_{out}$  the cutout speed. The coefficients  $a$ ,  $b$ , and  $c$  of a WT are calculated by solving the following linear system of equations:

$$\begin{aligned} a + b \cdot V_{in} + c \cdot V_{in}^2 &= 0 \\ a + b \cdot V_R + c \cdot V_R^2 &= P_R \\ a + b \cdot V_c + c \cdot V_c^2 &= P_R \cdot \frac{(V_c)^3}{(V_R)^3} \end{aligned} \quad (3)$$

where

$$V_c = \frac{V_{in} + V_R}{2}. \quad (4)$$

For a WT with  $P_R = 20$  kW having  $V_{in} = 3$  m/s,  $V_R = 11$  m/s and  $V_{out} = 22$  m/s, the obtained coefficients  $a$ ,  $b$ , and  $c$  are equal to 2.49,  $-1.74$ , and  $0.30$ , respectively.

### B. Load Demand FSPsN Model

Load model was implemented using database arcs and is depicted in Fig. 6. The imported data contain a vector named **Load** that consists of the 8760 values of hourly ac load expressed as a percentage of annual peak and comes from the IEEE-RTS [31]. Load is then calculated in  $p_{load3}$  by multiplying the resulted ratio,  $p_{load1}$ , with the annual peak demand,  $p_{in4}$ . Place  $p_{load5}$  sums the hourly load values; and thus, the annual load demand is estimated. The obtained value of  $p_{load5}$  at the end of a simulation year is used for the calculation of the energy index of unreliability (EIU). It has to be noticed that the IEEE-RTS annual load profile consists of 8736 values (364 days). In order to obtain 8760 hourly values, it is supposed that the load of the 365th day of the year is equal to the load of its previous week's same day (358th day of the year).

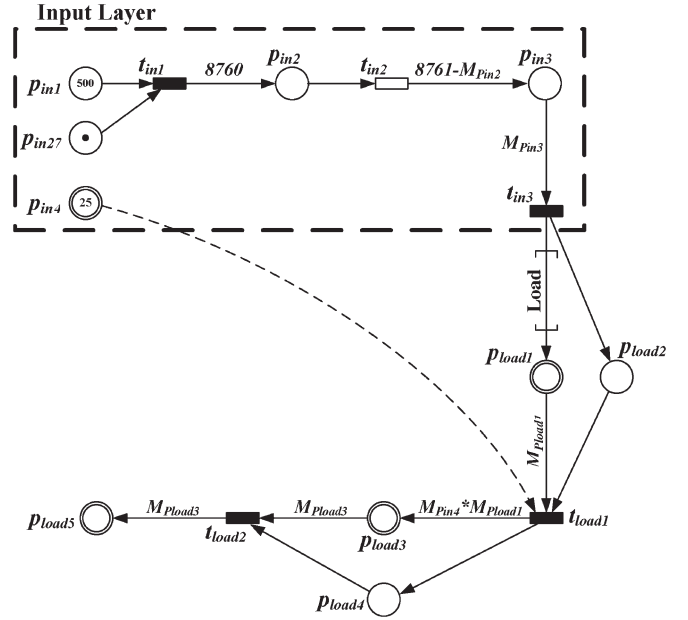


Fig. 6. Load demand FSPsN model using database arc.

### C. WT FSPsN Model

In wind data analysis, the wind speed is assumed to follow a Weibull distribution which requires knowledge of two parameters, namely: the shape factor  $k_W$  and the scale factor  $c_W$ . For wind data, a realistic value for the shape factor is  $k_W = 2$ , while an accurate approximation for the scale factor in a range of shape factors between 1.5 and 4 is given from [32]

$$c_W = 1.128 \cdot \bar{V}_{annual} \quad (5)$$

where  $\bar{V}_{annual}$  is the mean annual wind speed. For each hour  $i$  of the year, the wind speed at hub height  $V_i$  can be found by applying the inverse transform method in Weibull probability distribution [33]

$$V_i = c_W \cdot (-\ln(rnd(0, 1)))^{1/k_W} \quad (6)$$

where  $rnd(0, 1)$  is the uniformly distributed random number generation function in the interval  $(0, 1)$ . In the followed implementation, a value of 7 m/s for  $\bar{V}_{annual}$  at hub height has been assumed. Moreover, a forced outage rate of 4% for WT has been considered, with mean time to failure (MTTF) equal to 1920 h and mean time to repair (MTTR) equal to 80 h [2]. For both cases, the probability of time to failure (TTF) and time to repair (TTR) follows an exponential distribution, so both variables can be calculated using the inverse transform method [33] as follows:

$$TTF = -MTTF \cdot \ln(rnd(0, 1)) \quad (7)$$

$$TTR = -MTTR \cdot \ln(rnd(0, 1)). \quad (8)$$

After the calculation of TTF and TTR, the obtained values are rounded down to the nearest integer. In the proposed FSPN simulation, the random number generation for a variety of probability distributions is implemented by the proper arc weighting, using functions of the inverse transform method.

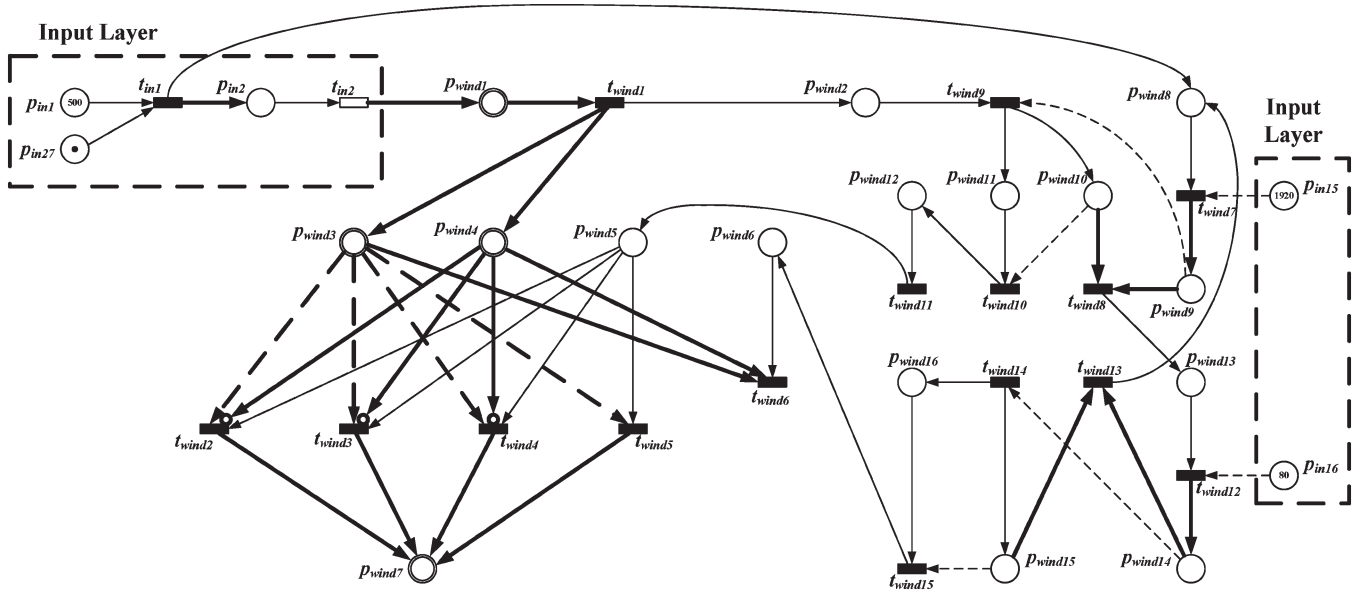


Fig. 7. WT FSPsN model.

TABLE II  
DESCRIPTION OF NONUNITARY WEIGHT ARCS IN WIND TURBINE FSPsN MODEL

Input	Output	Arc weight	Description of arc function
$t_{in1}$	$p_{in2}$	8760	Hours of the year
$t_{in2}$	$p_{wind1}$	$1.128 * M_{Pin6} * (-\ln(rnd(0, 1)))^{(1/M_{Pin5})}$	Calculation of wind speed
$t_{wind1}$	$p_{wind3}$	$M_{Pwind1}$	Transfer of $p_{wind1}$ value to $p_{wind3}$
$t_{wind1}$	$p_{wind4}$	$M_{Pwind1}$	Transfer of $p_{wind1}$ value to $p_{wind4}$
$p_{wind3}$	$t_{wind2}$	0	Lower bound of zero speed to $V_{in}$ interval (test arc)
$p_{wind3}$	$t_{wind3}$	$M_{Pin9}$	Lower bound of $V_{in}$ to $V_R$ interval (test arc)
$p_{wind3}$	$t_{wind4}$	$M_{Pin10}$	Lower bound of $V_R$ to $V_{out}$ interval (test arc)
$p_{wind3}$	$t_{wind5}$	$M_{Pin11}$	Lower bound of the interval containing wind speeds greater than $V_{out}$ (test arc)
$p_{wind3}$	$t_{wind6}$	$M_{Pwind3}$	Zeroing of place $p_{wind3}$ marking through sink transition $t_{wind6}$ firing
$p_{wind4}$	$t_{wind2}$	$M_{Pin9}$	Upper bound of zero speed to $V_{in}$ interval (inhibitor arc)
$p_{wind4}$	$t_{wind3}$	$M_{Pin10}$	Upper bound of $V_{in}$ to $V_R$ interval (inhibitor arc)
$p_{wind4}$	$t_{wind4}$	$M_{Pin11}$	Upper bound of $V_R$ to $V_{out}$ interval (inhibitor arc)
$p_{wind4}$	$t_{wind6}$	$M_{Pwind4}$	Zeroing of place $p_{wind4}$ marking through sink transition $t_{wind6}$ firing
$t_{wind2}$	$p_{wind7}$	0	WT energy produced in case that transition $t_{wind2}$ fires (eq. (2)(a))
$t_{wind3}$	$p_{wind7}$	$M_{Pin12} + M_{Pin13} * M_{Pwind3} + M_{Pin14} * M_{Pwind3}^2$	WT energy produced in case that transition $t_{wind3}$ fires (eq. (2)(b))
$t_{wind4}$	$p_{wind7}$	$M_{Pin8}$	WT energy produced in case that transition $t_{wind4}$ fires (eq. (2)(c))
$t_{wind5}$	$p_{wind7}$	0	WT energy produced in case that transition $t_{wind5}$ fires (eq. (2)(d))
$t_{wind7}$	$p_{wind9}$	$-M_{Pin15} * \ln(rnd(0, 1))$	Calculation of TTF for WT (eq. (6)) and update of place's $p_{wind9}$ marking
$p_{wind9}$	$t_{wind8}$	$M_{Pwind9}$	Zeroing of place $p_{wind9}$ marking when WT operation time is equal to TTF
$p_{wind10}$	$t_{wind8}$	$M_{Pwind9}$	Zeroing of place $p_{wind10}$ marking when WT operation time is equal to TTF
$t_{wind12}$	$p_{wind14}$	$-M_{Pin16} * \ln(rnd(0, 1))$	Calculation of TTR for WT (eq. (7)) and update of place's $p_{wind14}$ marking
$p_{wind14}$	$t_{wind13}$	$M_{Pwind14}$	Zeroing of place $p_{wind14}$ marking when WT repairing time is equal to TTR
$p_{wind15}$	$t_{wind13}$	$M_{Pwind14}$	Zeroing of place $p_{wind15}$ marking when WT repairing time is equal to TTR

The concept of utilizing arcs whose flow rates follow a given probability distribution is introduced in [29], in which the produced random variables were following general distributions.

The proposed FSPsN model is depicted in Fig. 7. For reader's convenience, the specific subnet has been simplified by hiding some of its implementation issues in order to emphasize its behavior. Moreover, the nonunitary arc weights of the WT FSPsN are represented bold. These arc weights are presented in Table II.

For each hour, the wind speed is calculated in  $p_{wind1}$  using (6), and the obtained value is transferred to  $p_{wind3}$  and  $p_{wind4}$ . These places are used for finding the WT power curve section that corresponds to the calculated wind speed according to (2) in case that WT is not in repairing condition. More specifically,  $p_{wind3}$  and its output test arcs are used for the inspection of the lower bound of WT power curve section, while  $p_{wind4}$  and its output inhibitor arcs are used for the inspection of the upper bound of WT power curve



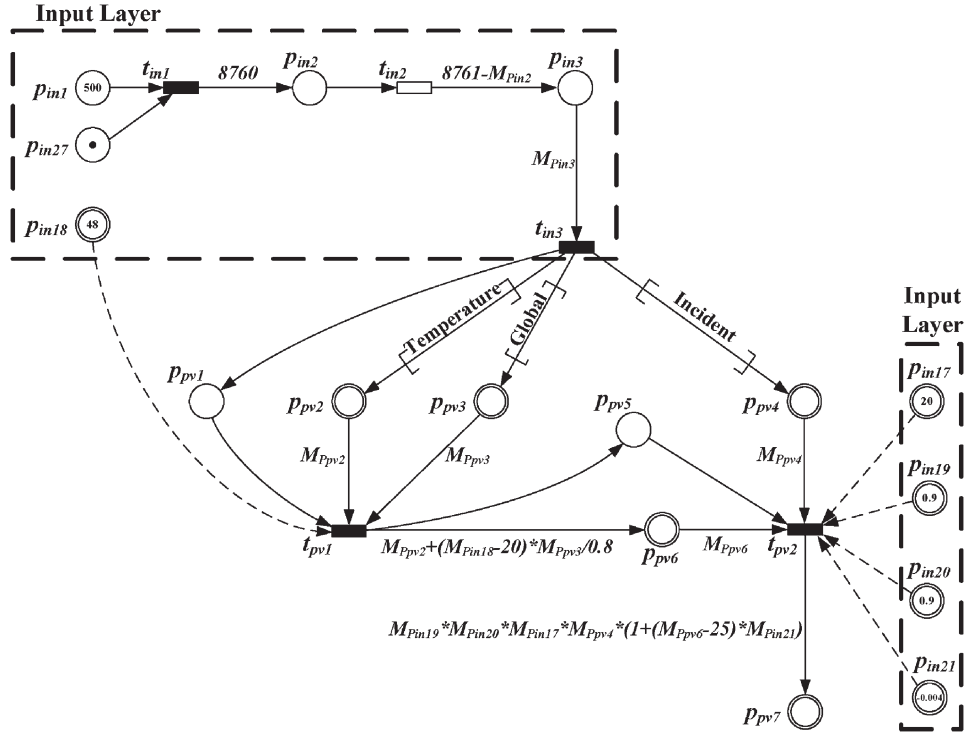


Fig. 8. PV FSPsN model using database arcs.

section. Firing of  $t_{wind2}$ ,  $t_{wind3}$ ,  $t_{wind4}$ , or  $t_{wind5}$  denote WT power production according to (2a), (2b), (2c), or (2d), respectively. The produced WT energy on an hourly base is shown in  $p_{wind7}$ .

The inspection for the operating and repairing state of the WT is performed in the right part of the FSPsN in Fig. 7. Places  $p_{wind9}$  and  $p_{wind14}$  show the TTF and TTR, respectively. This information is compared to the cumulative time of either operation or repair, which is computed in  $p_{wind10}$  or  $p_{wind15}$ , respectively. If the corresponding markings are equal,  $t_{wind8}$  or  $t_{wind13}$  fires and activates the opposite WT state ( $p_{wind13}$  or  $p_{wind8}$ ). In case that WT is in repair state,  $p_{wind5}$  is not activated; thus, there is no WT power production for the specific hour.

In case that the number of WTs is greater than one, different simulations for each WT have to be executed, even if all WTs are of the same type. This occurs because the variation of their corresponding failure and repair durations depends on the random number generation function [(7) and (8)]. The different WTs can be represented by different colors in the FSPsN of Fig. 7. More specifically, different colors will be used, namely: 1) in the part of the WT FSPsN that is included between transition  $t_{wind1}$  and place  $p_{wind7}$ ; and 2) in places  $p_{in7} - p_{in16}$  of the input layer FSPsN, which are related to the operational characteristics of the WTs.

#### D. PV FSPsN Model

In addition to the PV array, the PV FSPsN contains also an inverter, which converts dc electricity produced by the PV to ac

electricity needed by the load. The output of the PV array  $P_{PV}$  (in kW) is calculated from [34]

$$P_{PV} = n_{inv} \cdot f_{PV} \cdot P_{STC} \cdot \frac{G_A}{G_{STC}} \cdot (1 + (T_c - T_{STC}) \cdot C_T) \quad (9)$$

where  $n_{inv}$  is the inverter efficiency,  $f_{PV}$  is the PV derating factor,  $P_{STC}$  is the nominal PV array power in kW<sub>peak</sub> under standard test conditions (STC),  $G_A$  is the global solar radiation incident on the PV array in kW/m<sup>2</sup>,  $G_{STC}$  is the solar radiation under STC that is equal to 1 kW/m<sup>2</sup>,  $T_c$  is the temperature of the PV cells,  $T_{STC}$  is the STC temperature (25 °C), and  $C_T$  is the PV temperature coefficient in /°C. The PV derating factor is a scaling factor applied to the PV array output to account for losses, such as dust cover, aging, and unreliability of the PV array.  $T_c$  can be estimated from the ambient temperature  $T_a$  (in °C) and the global solar radiation on a horizontal plane  $G$  (in kW/m<sup>2</sup>) using (10) [35]

$$T_c = T_a + \frac{(NOCT - 20)}{0.8} \cdot G \quad (10)$$

where  $NOCT$  is the normal operating cell temperature, which is usually obtaining the value of 48 °C. The considered PV FSPsN is shown in Fig. 8, and its implementation requires the use of three database arcs. The first database arc imports hourly ambient temperature data in  $p_{pv2}$  from a vector named **Temperature**. The second database arc imports hourly global solar radiation data in  $p_{pv3}$  from a vector named **Global**. The third database arc imports hourly incident solar radiation data in  $p_{pv4}$  from a vector named **Incident**. All described input vectors contain 8760 hourly data values. The imported temperature

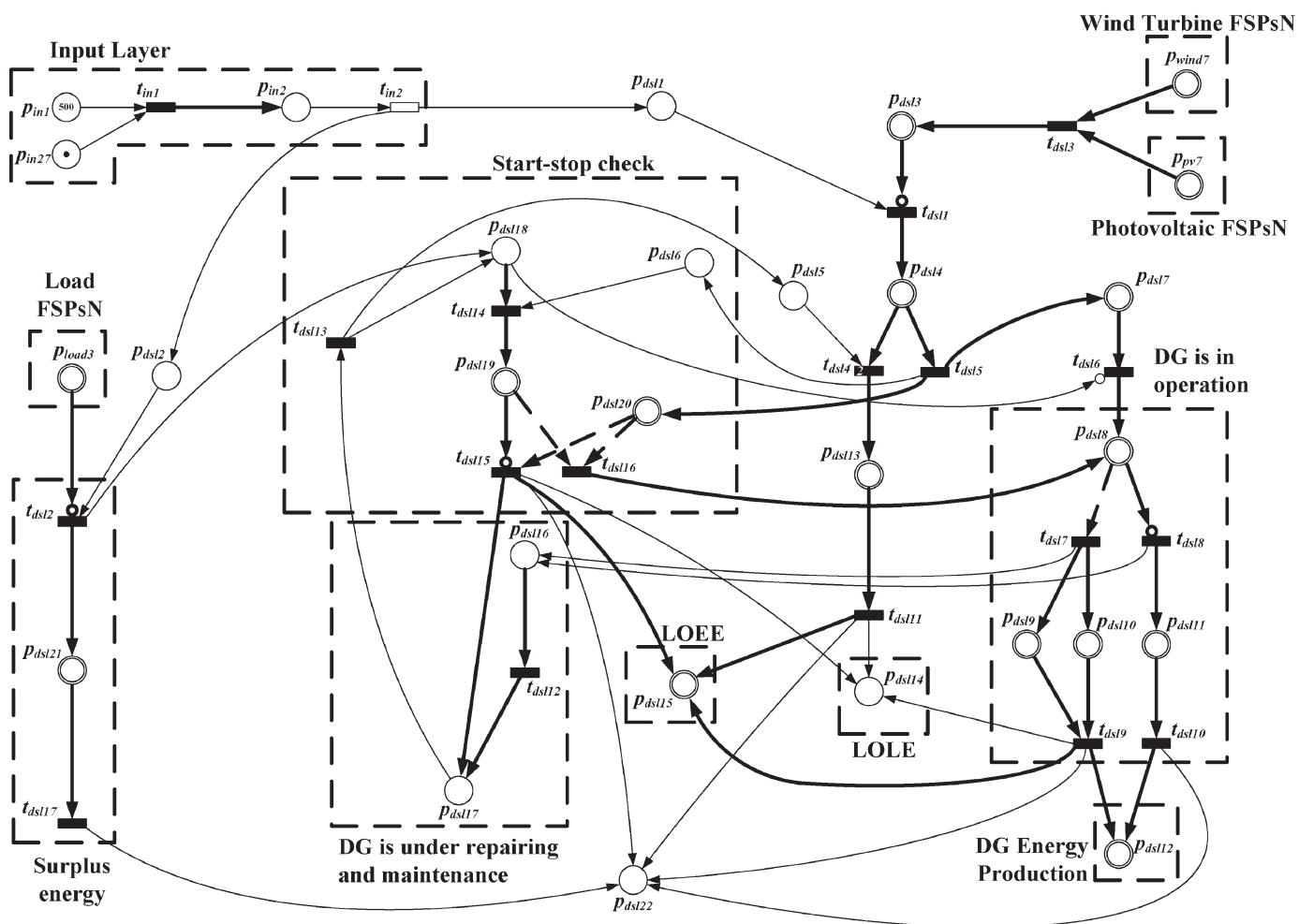


Fig. 9. Diesel generator FSPsN model.

The obtained PV FSPsN model is depicted in Fig. 8. Initially, the value of  $T_c$  is calculated in  $p_{pv6}$  using (10), and then this value is used to estimate  $P_{PV}$  in  $p_{pv7}$  using (9). Both transitions  $t_{pv1}$  and  $t_{pv2}$  that are used for these calculations are connected via test arcs with the appropriate places of the input layer FSPsN model.

#### E. Diesel Generator FSPsN Model

In the diesel generator FSPsN, an 18-kW diesel unit is modeled, which needs scheduled maintenance every 1000 h of operation. The duration of the maintenance follows uniform distribution in the hour interval  $[2, \dots, 24]$ . For each simulation hour, the studied SIPS is supposed to use all the available WT energy and PV energy to satisfy the load demand, while in the case that wind energy is not enough, the rest energy is supplied by the DG. Due to the expected large number of start-stop cycles of the diesel generator, a starting failure of 1% is included in the evaluation, while the repairing process follows the same distribution with the maintenance process. Fig. 9 presents a simplified version of the DG model in order to improve its

The DG FSPsN of Fig. 9 consists of two basic parts. In the first part, which is located in the left side of the model, the case that the produced energy from WT and PV is greater than load demand is developed. This condition enables  $t_{dsl2}$  and two basic events occur, namely: the information that the DG was not operating at the specific hour increases by one the marking of  $p_{dsl18}$ , while the excess energy production is calculated in  $p_{dsl21}$ . In the opposite case, the DG has to produce the necessary amount of energy in order to avoid capacity shortage. There are however more conditions that have to be examined before the DG operates. First, the DG cannot operate if a DG repair progress already exists. In this circumstance,  $p_{dsl5}$  has one token, and  $t_{dsl4}$  is enabled, leading the system to have unmet load that is calculated at  $p_{dsl13}$ , while  $p_{dsl15}$  shows the cumulative unmet load [loss of energy expectation (LOEE)] for the simulation year. Second, the case that DG was not working during the previous hour has to be examined. In this case,  $p_{dsl18}$  will have token(s), and  $t_{dsl14}$  will be enabled, which leads to the inspection of starting failure. Otherwise,  $t_{dsl6}$  will fire, leading to normal operation of DG.

Even if the DG is working properly for the specific hour, an additional contingency related with the magnitude of required

TABLE III  
DESCRIPTION OF NONUNITARY WEIGHT ARCS IN DIESEL GENERATOR FSPsN MODEL

Input	Output	Arc weight	Description of arc function
$t_{in1}$	$p_{in2}$	8760	Hours of the year
$p_{wind7}$	$t_{dsl3}$	$M_{p_{wind7}}$	Zeroing of place $p_{wind7}$ marking
$p_{pv7}$	$t_{dsl3}$	$M_{p_{pv7}}$	Zeroing of place $p_{pv7}$ marking
$t_{dsl3}$	$p_{dsl1}$	$M_{p_{wind7}} + M_{p_{pv7}}$	Total amount of WT and PV power
$p_{dsl3}$	$t_{dsl1}$	$M_{p_{load3}}$	Check if load is greater than WT and PV power production (inhibitor arc)
$t_{dsl1}$	$p_{dsl4}$	$M_{p_{load3}} - (M_{p_{wind7}} + M_{p_{pv7}})$	Calculation of the amount of power that DG has to produce
$p_{dsl4}$	$t_{dsl5}$	$M_{p_{dsl4}}$	Amount of power not served in case of DG repair
$p_{dsl4}$	$t_{dsl5}$	$M_{p_{dsl4}}$	Amount of power needed in case of start-stop check
$t_{dsl4}$	$p_{dsl13}$	$M_{p_{dsl4}}$	Power not served due to DG repair
$t_{dsl5}$	$p_{dsl7}$	$M_{p_{dsl4}}$	Amount of power needed in case that DG is operating
$p_{dsl7}$	$t_{dsl6}$	$M_{p_{dsl7}}$	Amount of power needed in case that DG is operating
$t_{dsl6}$	$p_{dsl8}$	$M_{p_{dsl7}}$	Amount of power that DG has to produce
$p_{dsl8}$	$t_{dsl7}$	$M_{p_{in22}}$	Check if needed power is greater than DG capacity (test arc)
$p_{dsl8}$	$t_{dsl8}$	$M_{p_{in22}}$	Check if needed power is less than DG capacity (inhibitor arc)
$t_{dsl7}$	$p_{dsl9}$	$M_{p_{in22}}$	The needed power is greater than CDG capacity, so the CDG is producing its maximum power
$t_{dsl7}$	$p_{dsl10}$	$M_{p_{dsl8}} - M_{p_{in22}}$	Amount of power that is greater from DG capacity (unmet load)
$t_{dsl8}$	$p_{dsl11}$	$M_{p_{dsl8}}$	Amount of power that DG is producing when needed power is less than DG capacity
$p_{dsl9}$	$t_{dsl9}$	$M_{p_{dsl9}}$	Produced power is equal to CDG capacity
$p_{dsl10}$	$t_{dsl9}$	$M_{p_{dsl10}}$	Unmet load
$p_{dsl11}$	$t_{dsl10}$	$M_{p_{dsl11}}$	Produced power from DG that satisfies load
$t_{dsl9}$	$p_{dsl12}$	$M_{p_{dsl9}}$	Energy produced, which is equal to DG capacity
$t_{dsl9}$	$p_{dsl15}$	$M_{p_{dsl10}}$	Addition of energy related to unmet load in LOEE
$t_{dsl10}$	$p_{dsl12}$	$M_{p_{dsl11}}$	Energy produced that satisfies load
$p_{dsl13}$	$t_{dsl11}$	$M_{p_{dsl13}}$	Power not served due to DG repair
$t_{dsl11}$	$p_{dsl15}$	$M_{p_{dsl13}}$	Loss of energy due to DG repair
$p_{dsl16}$	$t_{dsl12}$	$M_{p_{in23}}$	Comparison of DG operating hours with scheduled maintenance limit
$t_{dsl12}$	$p_{dsl17}$	$1 + M_{p_{in24}} + (M_{p_{in25}} - M_{p_{in24}}) * rnd(0, 1)$	Calculation of DG service duration due to scheduled maintenance
$p_{dsl18}$	$t_{dsl14}$	$M_{p_{dsl18}}$	Number of hours that DG has to operate
$t_{dsl14}$	$p_{dsl19}$	$rnd(0, 1)$	Random number generation for start-stop failure check
$p_{dsl19}$	$t_{dsl15}$	$M_{p_{in26}}$	Check if random number is less than starting failure probability (inhibitor arc)
$p_{dsl19}$	$t_{dsl16}$	$M_{p_{in26}}$	Check if random number is greater than starting failure probability (test arc)
$t_{dsl15}$	$p_{dsl15}$	$M_{p_{dsl20}}$	Addition of unmet load to LOEE
$t_{dsl15}$	$p_{dsl17}$	$1 + M_{p_{in24}} + (M_{p_{in25}} - M_{p_{in24}}) * rnd(0, 1)$	Calculation of DG service duration due to start-stop failure
$p_{load3}$	$t_{dsl2}$	$M_{p_{wind7}} + M_{p_{pv7}}$	Check if WT and PV power production is greater than load (inhibitor arc)
$t_{dsl2}$	$p_{dsl21}$	$(M_{p_{wind7}} + M_{p_{pv7}}) - M_{p_{load3}}$	Calculation of surplus energy production
$p_{dsl21}$	$t_{dsl27}$	$M_{p_{dsl21}}$	Amount of surplus energy production

load compared with the DG capacity has to be examined. If the required load (e.g., load demand minus WT and PV power) is greater than DG maximum power, a capacity shortage that is calculated at  $p_{dsl10}$  will occur; otherwise, all load demand will be satisfied (place  $p_{dsl11}$ ). The normal operation of DG (firing of  $t_{dsl7}$  or  $t_{dsl8}$ ) adds one token at  $p_{dsl16}$ . If its marking becomes equal to the duration of DG scheduled maintenance,  $t_{dsl12}$  will be enabled, the duration of DG repair will be calculated at  $p_{dsl17}$ , and at the end of the process a token will be added at  $p_{dsl18}$ .

As mentioned earlier, enabling of  $t_{dsl14}$  leads to the examination of DG starting failure case. A random number is generated at  $p_{dsl19}$  and is compared with DG starting failure probability of  $p_{in26}$ . If the produced number is greater than the failure probability the DG is working normally ( $t_{dsl16}$  fires); otherwise,  $t_{dsl15}$  is enabled, and DG is in repair, while the procedures followed are identical to those concerning the DG maintenance procedure after the firing of  $t_{dsl12}$ , described in the previous paragraph.

When the firing sequence for each hour has been completed, a token is added to  $p_{dsl22}$ , irrespective of the preceding firing

sequence. This ensures that the calculations in the DG model for the specific hour have been completed. Therefore, the role of  $p_{dsl22}$  is essential for the simulation running, as well as for the proper operation of the output layer FSPsN model at the end of a simulation year.

#### F. Output Layer FSPsN Model

The output layer FSPsN model calculates the remaining indexes that have not been evaluated in the WT FSPsN or in the DG FSPsN. Fig. 10 shows the part of the output layer model that estimates the annual value of the EIU index (place  $p_{out1}$ ), which is equal to the ratio of the annual LOEE and the annual load demand. Places  $p_{dsl15}$  and  $p_{load5}$  represent the annual values of LOEE and load, taken from the DG FSPsN and the load demand FSPsN, respectively. Transition  $t_{out1}$  can only be enabled if there are no remaining hours in the simulation year (i.e.,  $p_{in2}$  has no tokens), and simultaneously, the calculations in the DG model for the specific hour have been completed ( $p_{dsl22}$  has a token). After estimating EIU,  $t_{out2}$  fires and adds

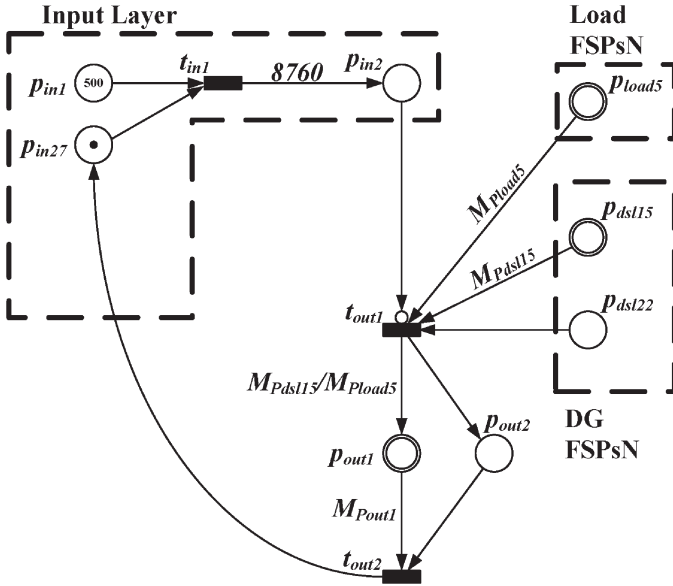


Fig. 10. Calculation of EIU index in output layer FSPsN model.

a token in  $p_{in27}$  in order to start the simulation process for the next year.

## VI. RESULTS

### A. FSPN Model Validation

In order to validate the results of the proposed FSPN model, a base scenario that contains one WT with a 20-kW rated power, a PV array of 20 kW<sub>peak</sub> and one DG with an 18-kW rated power has been considered to supply electric load that has an annual peak of 25 kW. The results of the proposed FSPN model are compared with the results of a Monte Carlo simulation that was implemented in MATLAB. The Monte Carlo simulation estimates the required indexes by simulating the actual process and random behavior of the system [36]. The occurrence of events that follow specific probability distributions is achieved using random numbers and converting them into density functions known to represent the behavior of the variables being considered. The use of Monte Carlo simulation for the reliability evaluation of power systems has been proven to be very efficient and accurate, especially in the case when complex operating conditions are involved, and/or the number of severe events is relatively large [33]. The proposed FSPN methodology, apart from the ability to represent the evolution of the simulation procedure graphically, differs from the Monte Carlo simulation in the way that the random events are modeled: instead of using well-known programming algorithms, the adopted methodology proposes a completely novel way of modeling based on the PN's specific features and properties.

To provide more reliable and accurate results for all the simulations, reliability and performance indexes are calculated for a simulation period of 500 years, and then they are averaged. The initial values of all input parameters are presented in Table I. Table IV summarizes the results obtained using the two simulation methods for the base scenario. Comparing the respective results obtained with the two methods, it is obvious

TABLE IV  
COMPARISON OF THE RESULTS OBTAINED BY THE FSPN MODEL AND MONTE CARLO SIMULATION METHOD FOR THE BASE SCENARIO

Index	FSPN	Monte Carlo	Difference (%)
LOLP (%)	7.38	7.23	2.07
LOLE (h/yr)	646.95	623.42	3.77
LOEE (kWh/yr)	2252.61	2105.99	6.96
EIU (%)	1.67	1.56	6.96
FOI (int/yr)	386.31	382.90	0.89
WEP (kWh)	59138	58389	1.28
SE (kWh)	14405	13970	3.11
CF (%)	33.76	33.33	1.29
DGEP (kWh)	61473	61934	-0.74

TABLE V  
INDEXES FOR THE BASE AND THE THREE ADDITIONAL SCENARIOS

Index	Base Scenario	First Scenario	Second Scenario	Third Scenario
LOLP (%)	7.38	6.59	8.54	3.66
LOLE (h/yr)	646.95	577.70	748.08	320.63
LOEE (kWh/yr)	2252.61	2151.88	2372.24	1718.63
EIU (%)	1.67	1.60	1.76	1.28
FOI (int/yr)	386.31	378.53	418.61	186.58
WEP (kWh)	59138	88305	42885	58955
SE (kWh)	14405	34931	8661	14386
CF (%)	33.76	33.60	24.48	33.65
DGEP (kWh)	61473	52933	71863	62172

that the proposed FSPN method provides almost identical results with Monte Carlo simulation method.

### B. Examination of Alternative Scenarios

This section investigates the flexibility and capabilities of the proposed FSPN methodology. Although the number of alternatives to the base scenario of Section VI-A is unlimited, due to space limitations three additional scenarios are performed. Initially, the effect of adding a smaller WT of 10-kW rated power is examined. The second scenario investigates the effect of lower wind potential in comparison with the base scenario. The third scenario examines the improvements of installing a larger DG of 22-kW rated power. In all cases mentioned, the durations that are associated with fault or repair of a WT or a DG are considered to have the constant values that were presented in Table I. These scenarios contain a combination of three components in SIPS (one dispatchable DG, together with two nondispatchable power sources, i.e., WTs and PVs), so these scenarios represent realistic and complicated case studies for SIPS, as can be seen in the bibliography [2], [37]–[40]. More specifically, [2], [37], and [38] study a SIPS that contains DG and WTs, [39] analyzes a SIPS that contains DG and PVs, while [40] studies a hybrid DG/WT/PV system.

The obtained results for all examined scenarios are summarized in Table V. The values of the base scenario are used as a benchmark for the additional scenarios.

In the first scenario, the addition of the second smaller WT has been implemented with the help of CPNs in the WT FSPsN and the input layer FSPsN. The input parameters that were changed in the newly added WT were places  $p_{in8}$  ( $P_{Rnew} = 10$  kW),  $p_{in12}$  ( $a_{new} = 1.25$ ),  $p_{in13}$  ( $b_{new} = -0.87$ ), and  $p_{in14}$  ( $c_{new} = 0.15$ ), while all other parameters remained



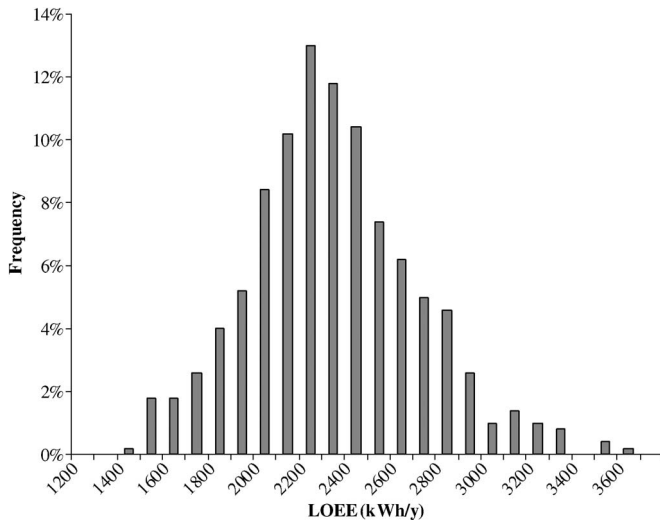


Fig. 11. LOEE distribution for the base scenario.

unchanged. From the comparison of the results of the base scenario and the first scenario in Table V, it is concluded that the addition of the second smaller WT improves slightly the reliability indexes. The main improvement is the significant reduction of the DG energy produced (DGEP) index, which shows that the DG is working less; thus, it consumes lower amounts of fuel. Moreover, the surplus energy is increased, and it may require the exploitation of this unused amount of energy (e.g., with water-pump systems).

In the second scenario, the mean value of the annual wind speed at hub height  $\bar{V}_{annual}$  is reduced from 7 to 6 m/s, in order to seek system's performance. As can be seen from Table V, all indexes in the second scenario deteriorate significantly compared to those of the base scenario which proves the dependence of system's performance on the wind potential.

In the third scenario, the rated power of DG is increased to 22 kW. This configuration produces much better results regarding the reliability indexes, while the increase of DGEP is negligible. The explanation is that the larger power of DG in this scenario allows better management of SIPS energy production in the cases that the power of DG at the base scenario was not adequate to meet the load demand. This conclusion can be explained by the fact that the increase of DGEP is almost equal to the decrease of LOEE.

The obtained information through the earlier analysis can produce histograms for all nine indexes and all scenarios of Table V. However, due to space limitations, only the LOEE histogram for the base scenario is presented in Fig. 11.

## VII. CONCLUSION

The advantages of the proposed FSPN methodology in the reliability analysis of hybrid SIPS are significant. First, the proposed methodology have presented the benefits of classical simulation methods, while it has the additional characteristic of the graphical representation of the simulation procedure that provides a powerful communication medium between theoreticians and practitioners. As a result, it is represented in the same

model the system's static structure, as well as its dynamically changing state.

Another major advantage of the proposed methodology is that a hierarchical PN method has been adopted for modeling of hybrid SIPS. In such a method, different levels of abstraction of the model are possible according to the needs of the person using the model, as some users need a very detailed view of specific parts of the model, while others need a more general and less detailed view of the overall system in order to study subsystems interaction. This allows the modeling of high complexity systems without the danger of having a very complicated model that is too difficult to represent and hard to understand. At the same time, the properties of the overall system can be obtained with respect to the properties of the subsystems that compose the overall system. This faces classical problems of PN modeling of complicated systems, such as state space explosion, and reduces significantly the computational complexity, while it can take advantage of modern methods, such as distributed simulation of systems. Moreover, the proposed methodology is of general use, as following a small number of well-defined steps, it can be adjusted to the specific needs, parameters, and characteristics of any system of this category independently of its topology and structural complexity. The calculation of a number of significant indexes makes possible the evaluation of alternative scenarios.

This paper also introduces a new type of PN arc called the database arc. This extension makes possible the use of real data in the simulation process, assuring the validity of the obtained results. From the presented analysis and discussion of the results, it has been shown that the proposed FSPN methodology is a very promising tool in reliability and performance evaluation of SIPS. Apart from the power systems area, which was considered in this paper, with rather few modifications and additions, the use of the proposed methodology may be further generalized to study systems from areas with similar characteristics with SIPS.

## REFERENCES

- [1] P. S. Georgilakis, "Technical challenges associated with the integration of wind power into power systems," *Renew. Sustainable Energy Rev.*, vol. 12, no. 3, pp. 852–863, Apr. 2008.
- [2] R. Karki and R. Billinton, "Cost effective wind energy utilization for reliable power supply," *IEEE Trans. Energy Convers.*, vol. 19, no. 2, pp. 435–440, Jun. 2004.
- [3] A. G. Bakirtzis, "A probabilistic method for the evaluation of the reliability of stand-alone wind energy systems," *IEEE Trans. Energy Convers.*, vol. 7, no. 1, pp. 99–107, Mar. 1992.
- [4] S. H. Karaki, R. B. Chedid, and R. Ramadan, "Probabilistic performance assessment of wind energy conversion systems," *IEEE Trans. Energy Convers.*, vol. 14, no. 2, pp. 217–224, Jun. 1999.
- [5] T. Murata, "Petri nets: Properties, analysis and applications," *Proc. IEEE*, vol. 77, no. 4, pp. 541–580, Apr. 1989.
- [6] K. Xing, M. C. Zhou, H. Liu, and F. Tian, "Optimal Petri-net-based polynomial-complexity deadlock-avoidance policies for automated manufacturing systems," *IEEE Trans. Syst., Man, Cybern. A, Syst., Humans*, vol. 39, no. 1, pp. 188–199, Jan. 2009.
- [7] J. Luo, W. Wu, H. Su, and J. Chu, "Supervisor synthesis for enforcing a class of generalized mutual exclusion constraints on Petri nets," *IEEE Trans. Syst., Man, Cybern. A, Syst., Humans*, vol. 39, no. 6, pp. 1237–1246, Nov. 2009.
- [8] A. L. Feller, T. Wu, D. L. Shunk, and J. Fowler, "Petri net translation patterns for the analysis of ebusiness collaboration messaging protocols," *IEEE Trans. Syst., Man, Cybern. A, Syst., Humans*, vol. 39, no. 5, pp. 1022–1034, Sep. 2009.

- [9] K. Jensen, *An Introduction to the Theoretical Aspects of Coloured Petri Nets*. New York: Springer-Verlag, 1994, pp. 230–272.
- [10] R. David and H. Alla, “Petri nets for modeling of dynamic systems—A survey,” *Automatica*, vol. 30, no. 2, pp. 175–202, Feb. 1994.
- [11] G. J. Tsinarakis, N. C. Tsourveloudis, and K. P. Valavanis, “Modeling, analysis, synthesis, and performance evaluation of multioperational production systems with hybrid timed Petri nets,” *IEEE Trans. Autom. Sci. Eng.*, vol. 3, no. 1, pp. 29–46, Jan. 2006.
- [12] K. S. Trivedi and V. G. Kulkarni, “FSPNs: Fluid stochastic Petri nets,” in *Proc. 14th Int. Conf. Appl. Theory Petri Nets*, 1993, pp. 24–31.
- [13] B. Tuffin, D. S. Chen, and K. S. Trivedi, “Comparison of hybrid systems and fluid stochastic Petri nets,” *Discr. Event Dyn. Syst.: Theory Appl.*, vol. 11, no. 1/2, pp. 77–95, Jan. 2001.
- [14] P. J. Haas, *Stochastic Petri Nets: Modelling, Stability, Simulation*. New York: Springer-Verlag, 2002.
- [15] W. G. Schneeweiss, “Tutorial: Petri nets as a graphical description medium for many reliable scenarios,” *IEEE Trans. Rel.*, vol. 50, no. 2, pp. 159–164, Jun. 2001.
- [16] J. Wang, Y. Deng, and G. Xu, “Reachability analysis of real time systems using time Petri nets,” *IEEE Trans. Syst., Man, Cybern. B, Cybern.*, vol. 30, no. 5, pp. 725–735, Oct. 2000.
- [17] K. L. Lo, H. S. Ng, and J. Trecat, “Power systems fault diagnosis using Petri nets,” *Proc. Inst. Elect. Eng.—Gener. Transm. Distrib.*, vol. 144, no. 3, pp. 231–236, May 1997.
- [18] P. S. Georgilakis, J. A. Katsigiannis, K. P. Valavanis, and A. T. Souflaris, “A systematic stochastic Petri net based methodology for transformer fault diagnosis and repair actions,” *J. Intell. Robot. Syst.*, vol. 45, no. 2, pp. 181–201, Feb. 2006.
- [19] N. Lu, J. H. Chow, and A. A. Descrochers, “A multi-layer Petri net model for deregulated electric power systems,” in *Proc. Amer. Control Conf.*, 2002, pp. 513–518.
- [20] H. Salefhar and T. Li, “Stochastic Petri nets for reliability assessment of power generating systems with operating considerations,” in *Proc. IEEE Power Eng. Soc. Winter Meeting*, 1999, pp. 459–464.
- [21] M. Dumitrescu, “Stochastic Petri nets architectural modules for power system availability,” in *Proc. Electron., Circuits Syst.*, 2002, vol. 2, pp. 745–748.
- [22] M. Gribaudo, A. Horváth, A. Bobbio, E. Tronci, E. Ciancamerla, and M. Minichino, “Fluid Petri nets and hybrid model-checking: A comparative case study,” *Reliab. Eng. Syst. Saf.*, vol. 81, no. 3, pp. 239–257, Sep. 2003.
- [23] R. Billinton and R. N. Allan, *Reliability Evaluation of Power Systems*, 2nd ed. New York: Plenum, 1996.
- [24] G. Ciardo, D. M. Nicol, and S. Trivedi, “Discrete-event simulation of fluid stochastic Petri nets,” *IEEE Trans. Softw. Eng.*, vol. 25, no. 2, pp. 207–217, Mar. 1999.
- [25] R. David and H. Alla, *Discrete, Continuous, and Hybrid Petri Nets*. Berlin, Germany: Springer-Verlag, 2005.
- [26] HOMER, *The Micropower Optimization Model*. [Online]. Available: <http://www.nrel.gov/homer>
- [27] HYBRID2, *The Hybrid System Simulation Code*. [Online]. Available: <http://www.ceere.org/rerl/projects/software/hybrid2/download.html>
- [28] J. Incera, R. Marie, D. Ros, and G. Rubino, “FluidSim: A tool to simulate fluid models of high-speed networks,” *Perform. Eval.*, vol. 44, no. 1–4, pp. 25–49, Apr. 2001.
- [29] K. Wolter, “Jump transitions in second order FSPNs,” in *Proc. MASCOTS*, Washington, DC, Oct. 1999, pp. 156–163.
- [30] Visual Object Net ++, *Petri Net Simulation Package*. [Online]. Available: [http://www.r-drath.de/VON/von\\_e.htm](http://www.r-drath.de/VON/von_e.htm)
- [31] C. Grigg, P. Wong, P. Albrecht, R. Allan, M. Bhavaraju, R. Billinton, Q. Chen, C. Fong, S. Haddad, S. Kuruganty, W. Li, R. Mukerji, D. Patton, N. Rau, D. Reppen, A. Schneider, M. Shahidepour, and C. Singh, “The IEEE Reliability Test System—1996,” *IEEE Trans. Power Syst.*, vol. 14, no. 3, pp. 1010–1020, Aug. 1999.
- [32] G. M. Masters, *Renewable and Efficient Electric Power Systems*. Hoboken, NJ: Wiley, 2004.
- [33] R. Billinton and W. Li, *Reliability Assessment of Electric Power Systems Using Monte Carlo Methods*. New York: Plenum, 1994.
- [34] M. Thomson and D. G. Infield, “Impact of widespread photovoltaics generation on distribution systems,” *IET Renew. Power Gener.*, vol. 1, no. 1, pp. 33–40, Mar. 2007.
- [35] T. Markvart and L. Castañer, *Practical Handbook of Photovoltaics: Fundamentals and Applications*. Oxford, U.K.: Elsevier, 2003.
- [36] P. Sarabando and L. C. Dias, “Multiattribute choice with ordinal information: A comparison of different decision rules,” *IEEE Trans. Syst., Man, Cybern. A, Syst., Humans*, vol. 39, no. 3, pp. 545–554, May 2009.
- [37] G. N. Kariniotakis and G. S. Stavrakakis, “A general simulation algorithm for the accurate assessment of isolated diesel-wind turbines systems interaction. Part II: Implementation of the algorithm and case-studies with induction generators,” *IEEE Trans. Energy Convers.*, vol. 10, no. 3, pp. 584–590, Sep. 1995.
- [38] S. A. Papathanassiou and M. P. Papadopoulos, “Dynamic characteristics of autonomous wind-diesel systems,” *Renew. Energy*, vol. 23, no. 2, pp. 293–311, Jun. 2001.
- [39] R. Billinton and R. Karki, “Reliability/cost implications of utilizing photovoltaics in small isolated power systems,” *Reliab. Eng. Syst. Saf.*, vol. 79, no. 1, pp. 11–16, Jan. 2003.
- [40] J. G. McGowan and J. F. Manwell, “Hybrid wind/PV/diesel system experiences,” *Renew. Energy*, vol. 16, no. 1, pp. 928–933, Jan. 1999.



**Yiannis A. Katsigiannis** was born in Athens, Greece, in 1975. He received the Diploma degree in production engineering and management, the M.S. degree, Diploma degree in environmental engineering, and the Ph.D. degree from the Technical University of Crete, Chania, Greece, in 2000, 2003, 2005, and 2008, respectively.

His research areas are renewable energy sources and their integration to power systems.

Dr. Katsigiannis is a member of the Technical Chamber of Greece.

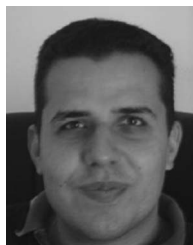


**Pavlos S. Georgilakis** (S'98–M'01) was born in Chania, Greece, in 1967. He received the Diploma degree in electrical and computer engineering and the Ph.D. degree from the National Technical University of Athens (NTUA), Athens, Greece, in 1990 and 2000, respectively.

He is currently Lecturer with the School of Electrical and Computer Engineering of NTUA. From 2003 to 2009, he was Assistant Professor with the Production Engineering and Management Department of the Technical University of Crete, Chania, Greece.

From 1994 to 2003, he was with Schneider Electric AE, where he was Research and Development Manager for three years. He is the author of two books, 40 papers in international journals, and 70 papers in international conference proceedings. His current research interests include design and analysis of renewable energy sources, as well as artificial intelligence and computer tools for power systems.

Dr. Georgilakis is a member of CIGRE and the Technical Chamber of Greece.



**George J. Tsinarakis** (M'06) received the B.S., M.S., and Ph.D. degrees from the Technical University of Crete, Chania, Greece, in 2000, 2002, and 2007, respectively.

His research interests include Petri nets theory, discrete event systems, modeling, supervisory control theory, analysis, performance evaluation, and optimization of production systems and manufacturing flexibility.